Published as: *Sci Signal*. ; 6(270): ra23–ra23.

LEAFY Controls Auxin Response Pathways in Floral Primordium Formation

Wuxing Li[1], **Yun Zhou**[1], **Xing Liu**[2,†], **Peng Yu**[2], **Jerry D. Cohen**[2], and **Elliot M. Meyerowitz**[1,3,*]

[1]Division of Biology, MC 156-29, California Institute of Technology, Pasadena, CA 91007, USA

[2]Department of Horticultural Science and Microbial and Plant Genomics Institute, University of Minnesota, Saint Paul, MN, 55108, USA

[3]Sainsbury Laboratory, Cambridge University, Bateman Street, Cambridge, CB2 1LR

Abstract

LEAFY is a transcription factor that acts as a master regulator of flowering and of flower development. It acts as a component of a switch that mediates the transition from the vegetative to the reproductive phase of plant development. Auxin is a plant hormone with many different roles in plant growth, including induction of new primordia of both leaves and flowers at the shoot apex. Here, we report that LEAFY acts in part by controlling the auxin response pathway in new primordia. Therefore, transcriptional master regulators of flower development and hormonal control of morphogenesis appear linked as interacting processes. We found that hormone perception not only controls, but is also controlled by, the transcriptional signals that create plant form.

Introduction

The aboveground development of plants is the result of the continued production of new leaf and flower primordia and new stem tissue, which form from a collection of stem cells at the tip of each shoot, called the shoot apical meristem (SAM). The formation of new leaves and flowers in the peripheral zone of the SAM is a result of locally increased concentration of the plant hormone auxin, application of which has long been known to induce new primordia (1). This increased auxin concentration results, at least in part, from regulated auxin transport mediated by the asymmetric distribution within SAM epidermal cells of proteins of the PIN-FORMED family of auxin efflux carriers. The subcellular localization of these auxin efflux carriers is regulated by the antagonistic functions of the kinase PINOID (PID) and phosphatase PP2A (2). This auxin distribution pattern, ultimately, results from the cellular interpretation of the physical forces created by expanding cells on their borders (3,

*To whom correspondence should be addressed: meyerow@caltech.edu.
†Current address: Division of Biology, MC 156-29, California Institute of Technology, Pasadena, CA 91007, USA.

WL and EMM conceived the project, WL, YZ, XL, YP performed the experiments, and WL and EMM wrote the manuscript.

The authors declare no conflict of interest.

4). Spatially and temporally regulated auxin biosynthesis also contributes to flower and leaf development (5, 6).

Auxin signal transduction is the result of a network of interactions between three types of cellular components (7). Auxin receptors interact with auxin and indole acetic acid (AUX/IAA) proteins such that binding of the hormone to the receptor triggers the degradation of the AUX/IAA proteins through a conserved degron. AUX/IAA proteins interact with AUXIN RESPONSE FACTORS (ARFs) to suppress their transcriptional regulation capability. Removal of AUX/IAA proteins, therefore, releases ARFs to either activate or suppress auxin-induced transcription. The AUX/IAA protein family of *Arabidopsis* has 29 members, and there are 23 ARF family members. These components exhibit different temporal and spatial patterns of expression, and specific AUX/IAA-ARF interaction pairs are major controls in tissue-specific auxin regulation pathways (8).

LEAFY (LFY) is a plant-specific transcription factor that integrates the environmental and internal signals that trigger the floral transition (9, 10). It functions by activating downstream meristem identity genes, such as *APETALA1*, which also serve as positive regulators of *LFY* expression – thereby creating a switch that irreversibly activates floral development (11). *LFY* is expressed in newly initiating floral primordia in their early developmental stages (12). LFY interacts with the auxin signaling pathway: LFY exhibits a genetic interaction with *pinoid* mutants and induces auxin-related genes (13–15). These results point to a role for LFY in the auxin-induced outgrowth of floral primordia, though *lfy*-null mutants do not cause severe defects in primordial formation or outgrowth. Thus, interactions between LFY-related processes and auxin signaling appear to exist, but their nature and importance remain unclear.

Results

Genetic interaction between LFY and PID

To learn more about the genetic pathways that interact with the LFY network during floral induction and flower development, we performed a genetic modifier screen in which more than 5,000 ethyl methanesulfonate (EMS)-mutagenized weak LFY loss-of-function *lfy-5* homozygous mutant seeds were grown and monitored for second-site enhancement or suppression of the *lfy-5* phenotype (16). Homozygous *lfy-5* plants have defective floral development, in which fewer than the normal number of petals and stamens are formed due to reduction in B-function homeotic gene activity, and in which increased numbers of secondary inflorescences develop, indicating a delay in specification of the SAM as an inflorescence, rather than a vegetative, meristem (16). One line of mutagenized *lfy-5* plants showed pin-like shoot apices (Fig. 1A, *pid-102 lfy-5*, and fig. S1A). The second-site mutation, named *pid-102*, when crossed away from *lfy-5*, had a phenotype similar to reported weak alleles of *pid* (Fig. 1A, *pid-102*, and fig. S1B), and map-based cloning and sequencing showed that this mutant was an R204K change in the PID protein (fig. S1C). Wild type plants of both *Landsberg* erecta and Wassilewskija ecotypes produce continuous leaves and flowers around the stems following a spiral phyllotactic pattern. This pattern is unaffected in *lfy-5*, *pid-102* or *pid-8* plants (Fig. 1A) (20). A mutant phenotype similar to that of the *pid-102 lfy-5* double mutant was observed in double mutants of either the weak

lfy-5 or the strong *lfy-6* mutant with *pid-8* (fig. S1 D and E), a weak loss-of-function allele of *PID* (14). The pin-like apices of the double mutants retain auxin responsiveness, because auxin application leads to lateral organs with floral characteristics (fig. S1 F).

LFY positively regulates auxin signaling

To better understand how loss of LFY function affects auxin pathways, we examined plants transgenic for both the PIN1 translational reporter *pPIN1::PIN1-GFP* and the synthetic auxin response reporter *pDR5rev::3XVenus-N7* (12, 17) in *lfy-5* and *lfy-5 pid-8* shoot apices. In wild-type plants PIN1-GFP has a polar localization toward incipient primordia (and then subsequently reverses to aim away from primordia as they develop), and production of 3XVenus-N7 from *pDR5rev::3XVenus-N7* marks incipient and developing floral primordia (12). The polarity of PIN1::GFP appeared unaffected in *lfy-5* SAMs, but the DR5 signal was significantly reduced compared to wild type (Fig. 1B; p=0.0003, Table S1). In *lfy-5 pid-8* double mutants, both PIN1-GFP and DR5 signals were reduced, and PIN1 did not appear polarized (Fig. 1B). These observations indicated that reduction of LFY function resulted in reduced auxin signaling output in the shoot apex.

To explore this further, we induced LFY overproduction using a dexamethasone-inducible *p35S::GVG-6XUAS::LFY* transgene (18), and found that dexamethasone caused a phenotype of abnormal inflorescence structure, altered floral development, and altered phyllotaxis in transgenic plants (fig. S2) (11). In addition, LFY induction strongly increased the signal from the *pDR5rev::3XVenus-N7* transgene at the sites of floral primordium formation (Fig. 1 C). This activation can also occur ectopically, because dexamethasone-treated *p35S::GVG-6XUAS::LFY* roots showed a significant increase in the *pDR5rev::3XVenus-N7* signal (p<0.001, fig. S3). Consistent with these results, expression of the AUX/IAA genes *IAA1*, *IAA17*, and *IAA29* were regulated by the *LFY* gene product (fig. S4 A and B). It is interesting to note that expression of *IAA29* was significantly increased in both *lfy* and *p35S::GVG-6XUAS::LFY* plants. Genes that respond in a similar way to both LFY overexpression and *lfy* loss-of-function might be candidates to help elucidate why overproduction of LFY results in a phenotype similar to *lfy* loss-of-function mutants (11, and this study).

LFY inhibits auxin biosynthesis

Reduced auxin signaling output in *lfy-5* could result from suppressed auxin signaling or of reduced auxin biosynthesis, or a combination of both. To discriminate between these possibilities, we measured the concentration of free IAA in wild-type and *lfy-6* shoot apices from which all but the earliest floral primordia had been dissected. The apices from *lfy-6* had a higher concentration (Fig. 2 A), which is inconsistent with the original hypothesis that *lfy* mutants have reduced auxin biosynthesis. Overexpression of LFY with the dexamethasone-inducible *p35S::GVG-6XUAS::LFY* reduced the concentration of IAA (Fig. 2B). The IAA concentration in the Ler-0 plants used for the analysis in Fig. 2A and the control Ler-0 plants used in Fig. 2B was different, and this difference may be due to that different batches of plants were used for sampling.

Furthermore, we examined the regulation of genes in the auxin biosynthesis pathway to see if LFY regulates their expression in a manner consistent with the inhibition of auxin biosynthesis. Consistent with the IAA analysis, examination of the expression of genes that function in the YUCCA pathway of auxin biosynthesis, *YUC1*, *YUC4*, *TAA1*, and *TAR2*, also suggested that LFY may inhibit this biosynthetic pathway in the shoot apex. Among the four genes tested, expression of *YUC4* and *TAR2* was significantly increased in *lfy-5* shoot apices compared to the expression in the shoot apices of wild-type Ler-0 plants (Fig. 2 C and D). With a dexamethasone-inducible *p35S::GVG-6XUAS::LFY* transgenic line (Fig. 2E), we found that the expression of *YUC1* and *YUC4* was reduced by more than 2 fold within 4 hours of dexamethasone treatment (Fig. 2 F and G). Four hours of LFY induction did not reduce *TAA1* and *TAR2* expression, but *TAR2* expression was reduced to 56% of that of the mock treatment after 12 hours of induction (fig. S4 C and D). In addition, LFY bound to the *YUC4* genomic region (+1749–1998 bp, A in the start codon ATG as +1), which suggests a direct role for LFY in regulating *YUC4* expression (Fig. 2H). The data, therefore, favor the hypothesis that auxin signaling in flower primordia is reduced in *lfy* mutants, even in the presence of increased auxin concentration and auxin biosynthesis.

Auxin stimulates LFY expression

We analyzed the dynamics of *LFY* expression and auxin signaling by live imaging of the expression of *pDR5rev::3XVenus-N7* and of *pLFY::GFP-ER* in developing shoot apices (Fig. 3 A and B, fig. S5). The appearance of DR5 signal preceded LFY reporter signal in developing flower primordia, suggesting that auxin signaling increases prior to the onset of *LFY* expression. The LFY reporter signal was consistently reduced in *lfy-5 pid-8*, *pin1-1*, and *pid-4* mutant backgrounds (Fig. 3 C–E), making it possible that auxin signaling stimulates *LFY* expression. To verify the ability of auxin to stimulate *LFY* expression, we tested the response of *pLFY::GFP-ER* in roots, where *LFY* is normally not expressed (Fig. 3F) and found that 24 hours after the addition of the auxin NAA, the LFY reporter was visible in root epidermal and pith cells (Fig. 3G). This induction of the LFY reporter was suppressed by inclusion of cycloheximide, indicating that de novo protein synthesis was required (Fig. 3H). These data suggested a role for auxin in promoting, or derepressing, *LFY* transcription.

LFY inhibits its own expression

LFY overexpression reduced endogenous *LFY* promoter activity by about 3 fold (Fig. 2I). Consistent with this, the *LFY* transcript was more abundant (fig. S4 E) in the shoot apices of *lfy-5* mutant plants. In addition, in comparison with that in wild-type plants (Fig. 3I), the intensity of the LFY reporter signal from *pLFY::GFP-ER* was greater in *lfy-5* mutants (Fig. 3J), indicating a higher *LFY* promoter activity in a *lfy* loss-of-function background. Furthermore, ChIP-seq data indicate that LFY can bind to its own promoter region (13, 15). Thus, it appears that, during the floral transition, auxin may increase *LFY* transcription, and that LFY has a positive role in promoting auxin signaling, which may lead in turn to a further increase in *LFY* activity (Fig. 4). A counterbalancing effect is the negative influence of LFY activity on auxin biosynthesis through the YUCCA pathway, and the repressive effect of LFY on its own promoter.

Discussion

LFY is a master regulator that functions in switching on floral development. High-throughput techniques, including microarray, ChIP-seq, and ChIP-ChIP, have suggested the involvement of LFY in auxin regulation, a hormonal regulation system critical for multiple developmental programs (13, 15). In this study, we present genetic and live-imaging data indicating that LFY has a positive role in the auxin signaling pathway and may exert a negative function in the auxin biosynthesis pathway. Our data also indicated that during floral primordium formation, *LFY* expression occurred temporally after auxin signaling, and that *LFY* was activated by auxin. In addition, we found that LFY had a negative role in regulating its own expression. Taken together, these data suggest that LFY might be involved in one positive and two negative feedback loops in the control of the auxin biosynthesis and auxin signaling pathways (Fig. 4).

Additionally, we found that auxin signaling both controlled, and was controlled by, the transcriptional signals that regulate the appearance and early development of flowers. This interrelation of hormone function with a key transcriptional regulator raises the question of how frequently similar interactions may explain specific hormonal effects, and also, also the question of the degree to which the functions of transcriptional master regulators involve hormone systems. These studies also raise questions about the evolutionary history of this interaction between an ancient regulatory gene and an ancient hormone signaling pathway.

Materials and Methods

Plant materials

The weak *lfy-5* allele used for genetic modifier screening was previously described (10). Other mutant alleles including *lfy-6*, *pid-8*, *pid-4*, and *pin1-1* have also been reported (10, 19, 20). Marker lines including *pPIN1::PIN1-GFP pDR5rev::3xVenus-N7* and *pLFY::GFP-ER* were previously reported (12). These markers carry antibiotic resistance and plants were screened on half-MS plates supplemented with 50 mg/L kanamycin (*pPIN1::PIN1-GFP* marker), 25 mg/L Basta (*pDR5rev::3XVenus-N7*), or 35 mg/L gentamycin (For *pLFY::GFP-ER*). Genotyping with gene or allele-specific primers (Table S2) was performed when needed for construction or phenotypic analysis of multiple mutants. Plants were grown under constant light at 22°C.

Construction of vectors, transformation, and transformant analysis

For *pLFY::LFY-eGFP* construction, a 3.4 Kb promoter fragment upstream of the start codon was amplified from genomic DNA and inserted into a pBJ36 shuttle vector. The *LFY* coding sequence was amplified from cDNA obtained from inflorescence shoots of wild type Col-0 plants, and the enhanced green fluorescent protein (eGFP) coding sequence added to its 3′ end by ligation PCR. The *cLFY-eGFP* fragment was then inserted into the pBJ36 shuttle vector downstream of the *pLFY* sequence (21). The finalized *pLFY::cLFY-eGFP* was then transferred into pMLBART binary vector with NotI sites. Confirmed binary vector DNA was transformed into Ler-0 and *lfy-6*/+ by the floral dip method (22). Transformants were screened on MS plates supplemented with 25 mg/L Basta and lines that both showed

expression patterns consistent with previously reported *pLFY::GFP-ER* or in situ hybridization results and that rescued the *lfy-6* mutation were used for further experiments.

For *p35S::GV-6XUAS::LFY* construction, a *LFY* coding sequence with gateway-compatible ends was amplified from cDNA obtained from inflorescence shoots of wild type Col-0 plants, and was then incorporated into the pTA7002 binary vector with LR reaction. Confirmed binary vector was transformed into wild type Ler-0 plants and *pPIN1::PIN1-GFP pDR5rev::3XVenus-N7* double marker lines. Transformants were screened with B5 media supplemented with 35 mg/L hygromycin.

Microscopy

Confocal microscopy was performed with a Zeiss LSM 510 microscope. For live imaging, developing floral buds were removed from plants and they were grown in a wet box, with images taken periodically using a water-dipping lens (12). For observation of the effect of dexamethasone treatment, 20 μl of 20 μM dexamethasone in 0.05% DMSO was applied to the shoot apex, and imaging was done at scheduled time points with the exactly same settings at each point. For mock treatment, 20 μl 0.05% DMSO was applied. For observing fluorescence markers, shoot apices freshly detached from plants were used as previous described (23). When needed, FM4-64 staining to visualize cell membranes was performed by applying 20 μl of 5 mg/L FM4-64 in water onto the shoot apex with developing floral buds removed, with unbound dye washed away with distilled water after 5 minutes of staining at room temperature. Images were processed with Zeiss LSM 510 software. Dissecting microscopy was performed using a Zeiss Stemi SV11 dissecting scope. Sizes were measured by imaging a standard ruler at the same setting as used for imaging plant organs.

For root experiments, seeds homozygous for *pLFY::GFP-ER* (12) or *pLFY::cLFY-eGFP* transgenes were sown on ½ MS media and 7-d old seedlings were transferred to ½ MS supplemented with either a mock treatment solution (0.01% DMSO), 10 μM NAA, or 10 μM NAA + 10 μM cycloheximide. For cycloheximide treatment, seedlings were pretreated by flushing briefly with 10 μM cycloheximide and then left for 2 hours before being transferred onto plates. Imaging was performed after 24 hours of treatment.

Quantification of the DR5 signals in representative images of the l*fy-5* and wild-type SAMs was performed using Image J (http://rsbweb.nih.gov/ij/). Each raw data file of a stack of images was subjected to a Z-project function, with “MAX intensity” selected for image projection. Only the incipient primordial sites in wild-type and mutant SAMs were used for quantification. The primordial sites were enlarged with the “Square” then “Image-Zoom-To selection” functions. To measure the signal intensity, the inner portion of the nuclei, where DR5 signal is located, was marked with the “circle” function and the mean value of the signal intensity was obtained with the “Analyze-Histogram” function. The final readings of the mean signal intensity range from a minimum of 0 to a maximum of 4095. The background was subtracted with the Process- Subtract background function. Results from signal intensity quantification of 5 images of wild-type SAMs and 6 images of *lfy-5* SAMs were analyzed. All images were taken with the same setting.

Quantitative RT-PCR

Unless otherwise noted, plant materials used for quantitative reverse transcriptase-(RT)-PCR were young inflorescence apices with developing floral buds up to stage 4. Plant RNA extraction was performed with Qiagen RNAeasy kit following manufacturer's instructions. For reverse transcription, 1 μg of RNA was pretreated with Invitrogen RNA-free DNase, and then subjected to reverse transcription with Superscript II kit. Quantitative PCR was performed with a LightCycler® 480 cycler following the instruction manual. See table S2 for a list of primers used for quantitative PCR. For most experiments excepting noted below, at least three biological replicates were included. For each biological replicate, three technical replicates were performed for quantitative PCR. Results were analyzed with an absolute quantitative approach with the LightCycler® 480 software. A standard curve test was performed for each gene specific primer pair using series dilutions of control cDNA from Ler-0 shoot apices, and concentration of samples was derived from the standard curve. The derived concentrations were normalized with the expression of *ACTIN2* as an internal control. Results were subject to Wilcoxon ranksum test for equal medians with MATLAB R2011B (MathWorks, USA).

Free IAA quantification

For determining free IAA concentrations in shoot apices, shoot tips with young floral buds up to stage 3, from inflorescence shoots with length ranges between 2 cm and 5 cm, were used. Older floral buds and stem tissues were removed with a spring scissors (Fine Science Tools, cat. no. 91500-09). Five biological replicates were prepared for each of the Ler-0 and *lfy-6* genotypes. For testing the effect LFY overexpression on auxin biosynthesis, the third generation of transgenic plants homozygous to the *p35S::GVG-6XUAS::LFY* transgene were used. Both Ler-0 and transgenic plants grown under the same conditions were subjected to no treatment, or either mock treatments (0.05% v/v DMSO), or DEX (20 μM DEX in 0.05% v/v DMSO) for 24 hours with a floral dipping approach. Sampling was similar to that previously described and five independent replicates were collected for free IAA quantification. For each replicate, 3–15 mg of fresh tissue was weighted, frozen in liquid nitrogen, and stored at −80°C. For each sample, 20 μL of homogenization buffer (35% of 0.2 M imidazole and 65% isopropanol, pH 7.0) containing 0.2 ng of [$^{13}C_6$]IAA was added before homogenization. The amount of free IAA was analyzed by micro-scale solid phase extraction followed by gas chromatography–selected reaction monitoring–mass spectrometry on a Thermo Trace GC Ultra coupled to a TSQ Vantage triple quadrupole MS system (Thermo Scientific) as previously described (24, 25).

Yeast one hybrid assay

For Y1H experiments, the *YUC4* genomic regions used were selected based on the presence of putative LFY binding sites according to the consensus LFY binding sequences as suggested by Winter *et al.* and Moyroud *et al.* (13, 15). These genomic regions (about 250 bp in length) were PCR amplified and cloned into pLacZi bait vectors containing a LacZ reporter gene, and *LFY* cDNA was fused to the GAL4 activation domain (GAL4-AD) in a pDEST22 vector (Invitrogen). The two vectors were transformed into the yeast strain YM4271 (Clontech), and the DNA-protein interaction was determined by the quantification

of β-galactosidase activity in triplicate experiments. In a parallel experiment, empty GAL4-AD vector combined with *YUC4* promoter fragments in pLacZ was included as a negative control.

Supplementary Material

Refer to Web version on PubMed Central for supplementary material.

Acknowledgments

We thank members of the Meyerowitz lab for comments and discussion. We thank Adrienne Roeder for technical assistance with mapping, Zachary Nimchuk for technical assistance with construct preparation, Vijay Chickarmane for assistance in statistical analysis, Marcus Heisler for technical assistance with imaging, and Arnavaz Garda for plant care. We thank Yuichiro Watanabe for the *pTA7002* binary vector and The Arabidopsis Information Resource (TAIR) for essential genome information. Work at the California Institute of Technology was supported by the Department of Energy Office of Basic Energy Sciences, Division of Chemical Sciences, Geosciences and Biosciences grant DE-FG02-88ER13873 (EMM). Work at the University of Minnesota was supported by the National Science Foundation (grants MCB-0725149, IOS-PGRP-0923960, IOS-PGRP-1238812 and MCB-1203438), the Minnesota Agricultural Experiment Station, and the Gordon and Margaret Bailey Endowment for Environmental Horticulture.

References and Notes

1. Snow M, Snow R. Auxin and leaf formation. New Phytol. 1937; 36
2. Michniewicz M, Zago MK, Abas L, Weijers D, Schweighofer A, Meskiene I, Heisler MG, Ohno C, Zhang J, Huang F, Schwab R, Weigel D, Meyerowitz EM, Luschnig C, Offringa R, Friml J. Antagonistic regulation of PIN phosphorylation by PP2A and PINOID directs auxin flux. Cell. 2007; 130:1044–1056. [PubMed: 17889649]
3. Heisler MG, Hamant O, Krupinski P, Uyttewaal M, Ohno C, Jonsson H, Traas J, Meyerowitz EM. Alignment between PIN1 polarity and microtubule orientation in the shoot apical meristem reveals a tight coupling between morphogenesis and auxin transport. PLoS Biol. 2010; 8
4. Nakayama N, Smith R, Mandel T, Robinson S, Kimura S, Boudaoud A, Kuhlemeier C. Mechanical regulation of auxin-mediated growth. Curr Biol. 2012; 22:1468–1476. [PubMed: 22818916]
5. Cheng YF, Dai XH, Zhao YD. Auxin synthesized by the YUCCA flavin Monooxygenases is essential for embryogenesis and leaf formation in *Arabidopsis*. Plant Cell. 2007; 19:2430–2439. [PubMed: 17704214]
6. Zhao YD. Auxin biosynthesis and its role in plant development. Annu Rev Plant Biol. 2010; 61:49–64. [PubMed: 20192736]
7. Mockaitis K, Estelle M. Auxin receptors and plant development: a new signaling paradigm. Annu Rev Cell Dev Biol. 2008; 24:55–80. [PubMed: 18631113]
8. Lau S, Jurgens G, De Smet I. The evolving complexity of the auxin pathway. Plant Cell. 2008; 20:1738–1746. [PubMed: 18647826]
9. Blazquez MA, Ferrandiz C, Madueno F, Parcy F. How floral meristems are built. Plant Mol Biol. 2006; 60:855–870. [PubMed: 16724257]
10. Weigel D, Alvarez J, Smyth DR, Yanofsky MF, Meyerowitz EM. LEAFY controls floral meristem identity in *Arabidopsis*. Cell. 1992; 69:843–859. [PubMed: 1350515]
11. Wagner D, Sablowski RWM, Meyerowitz EM. Transcriptional activation of APETALA1 by LEAFY. Science. 1999; 285:582–584. [PubMed: 10417387]
12. Heisler MG, Ohno C, Das P, Sieber P, Reddy GV, Long JA, Meyerowitz EM. Patterns of auxin transport and gene expression during primordium development revealed by live imaging of the *Arabidopsis* inflorescence meristem. Curr Biol. 2005; 15:1899–1911. [PubMed: 16271866]
13. Winter CM, Austin RS, Blanvillain-Baufume S, Reback MA, Monniaux M, Wu MF, Sang Y, Yamaguchi A, Yamaguchi N, Parker JE, Parcy F, Jensen ST, Li HZ, Wagner D. LEAFY target

genes reveal floral regulatory logic, cis motifs, and a link to biotic stimulus response. Dev Cell. 2011; 20:430–443. [PubMed: 21497757]

14. Ezhova TA, Soldatova OP, Kalinina AY, Medvedev SS. Interactions between the *ABRUPTUS*/*PINOID* and *LEAFY* genes during floral morphogenesis in *Arabidopsis thaliana* (L.) Heynh. Russ J Genet. 2000; 36:1418–1422.
15. Moyroud E, Minguet EG, Ott F, Yant L, Pose D, Monniaux M, Blanchet S, Bastien O, Thevenon E, Weigel D, Schmid M, Parcy F. Prediction of regulatory interactions from genome sequences using a biophysical model for the *Arabidopsis* LEAFY transcription factor. Plant Cell. 2011; 23:1293–1306. [PubMed: 21515819]
16. Wagner D, Meyerowitz EM. SPLAYED, a novel SWI/SNF ATPase homolog, controls reproductive development in *Arabidopsis*. Curr Biol. 2002; 12:85–94. [PubMed: 11818058]
17. Ulmasov T, Murfett J, Hagen G, Guilfoyle TJ. Aux / IAA proteins repress expression of reporter genes containing natural and highly active synthetic auxin response elements. Plant Cell. 1997; 91(11):1963–1971. [PubMed: 9401121]
18. Aoyama T, Chua NH. A glucocorticoid-mediated transcriptional induction system in transgenic plants. Plant J. 1997; 11:605–612. [PubMed: 9107046]
19. Okada K, Ueda J, Komaki MK, Bell CJ, Shimura Y. Requirement of the auxin polar transport-system in early stages of *Arabidopsis* floral bud formation. Plant Cell. 1991; 3:677–684. [PubMed: 12324609]
20. Bennett SRM, Alvarez J, Bossinger G, Smyth DR. Morphogenesis in *pinoid* mutants of *Arabidopsis thaliana*. Plant J. 1995; 8:505–520.
21. Dubrovsky JG, Sauer M, Napsucialy-Mendivil S, Ivanchenko MG, Friml J, Shishkova S, Celenza J, Benkova E. Auxin acts as a local morphogenetic trigger to specify lateral root founder cells. Proc Natl Acad Sci USA. 2008; 105:8790–8794. [PubMed: 18559858]
22. Clough SJ, Bent AF. Floral dip: a simplified method for *Agrobacterium*-mediated transformation of *Arabidopsis thaliana*. Plant J. 1998; 16:735–743. [PubMed: 10069079]
23. Reddy GV, Heisler MG, Ehrhardt DW, Meyerowitz EM. Real-time lineage analysis reveals oriented cell divisions associated with morphogenesis at the shoot apex of *Arabidopsis thaliana*. Development. 2004; 131:4225–4237. [PubMed: 15280208]
24. Liu X, Cohen JD, Gardner G. Low-Fluence Red light increases the transport and biosynthesis of auxin. Plant Phys. 2011; 157:891–904.
25. Liu X, Hegeman AD, Gardner G, Cohen JD. Protocol: High-throughput and quantitative assays of auxin and auxin precursors from minute tissue samples, in. Plant Methods. 2012; 8:31. [PubMed: 22883136]

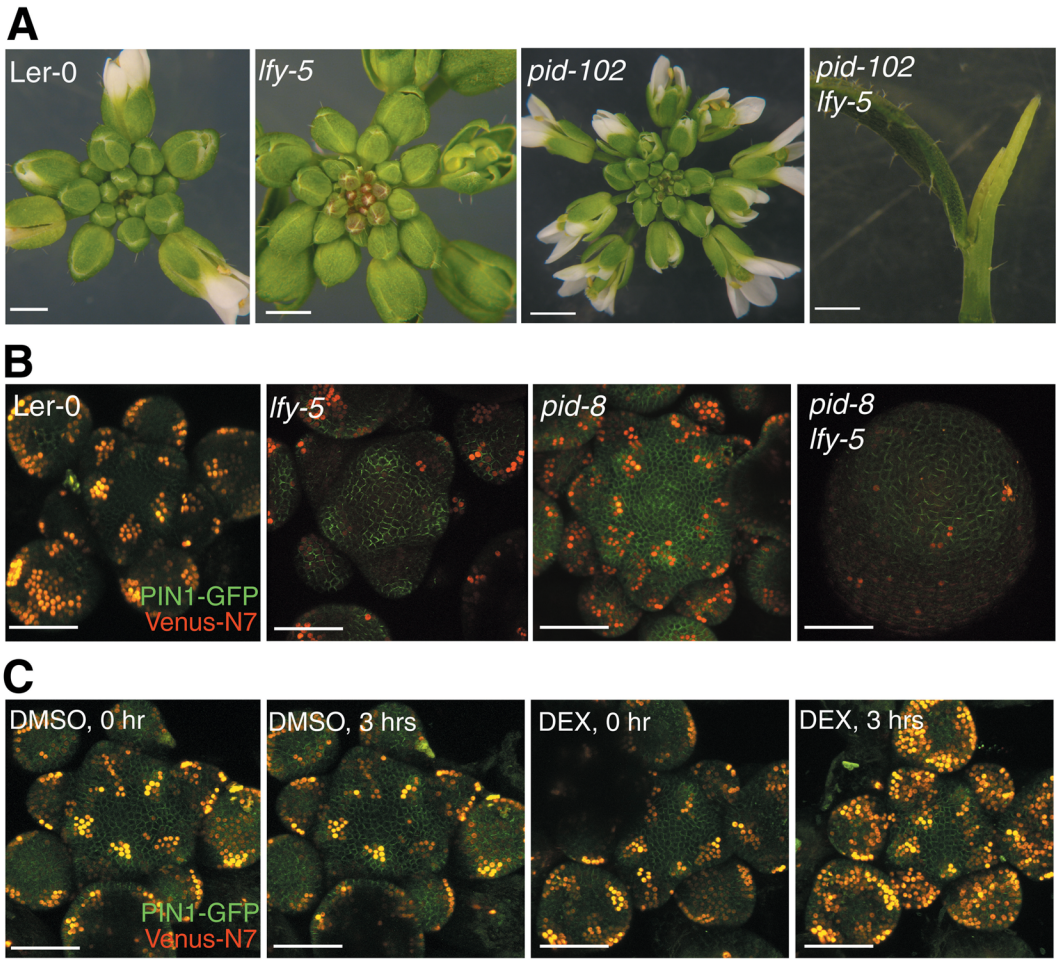

Fig. 1. The *lfy*, *pid*, and double mutant phenotypes and imaging of auxin signaling and PIN localization using reporters in developing floral buds

(**A**) Inflorescence apices of wild type (Ler-0) and the *lfy-5* and the *pid-102* mutants show the similar phyllotactic patterns. The double mutant *pid-102 lfy-5* shows reduced apical dominance, reduced shoot apical meristem activity, and increased branching. Bar in A represents 1 mm.

(**B**) The auxin efflux reporter PIN1-GFP (green) produced from *pPIN1::PIN1-GFP* and the DR5 auxin signaling reporter (red) produced from *pDR5rev::3XVenus-N7* is shown in the plants of the indicated genotypes.. See table S1 for statistical analysis of DR5 intensity in wild-type and *lfy-5* SAMs.

(**C**) The effect of *LFY* overexpression on the DR5 and PIN1-GFP signals. Shown are the shoot apices of *pPIN1::PIN1-GFP pDR5rev::3XVenus-N7 35S::GVG-6XUAS::LFY* plants. The first two images show the signals from the SAMs of a plant before and after 3 hours of mock (DMSO) treatment. The second pair of images shows the SAMs of a plant before and after 3 hours of dexamethasone (DEX) treatment. Images in panels B and C are representatives of 30 or more observed SAMs. Bars in B–C, 50 μm.

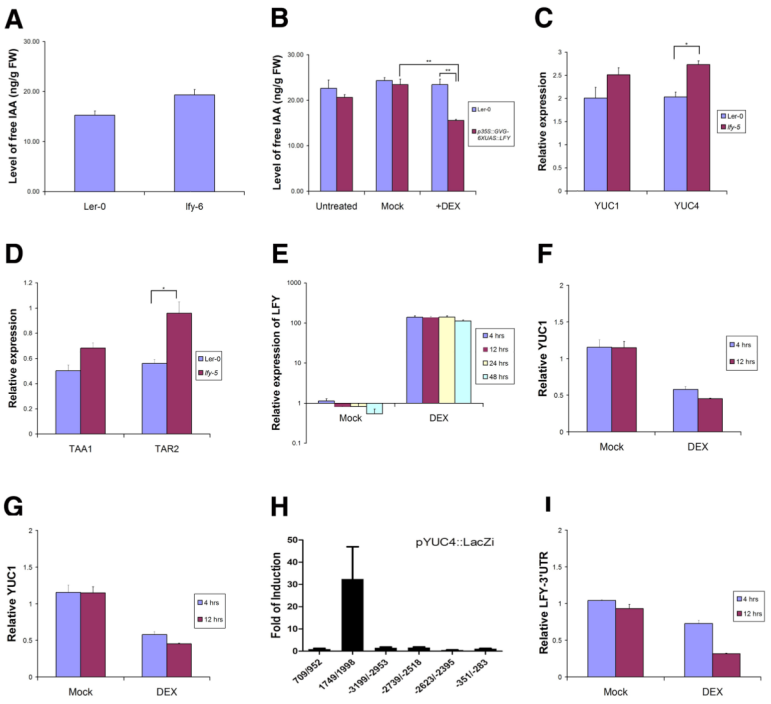

Fig. 2. Free IAA amount and expression of auxin biosynthesis genes

(**A**) Free IAA quantified from 3–8 mg fresh weight inflorescence apices from of Ler-0 and *lfy-6* plants (n=5 for each genotype).

(**B**) Free IAA quantified from 8–15 mg fresh weight inflorescence apices of Ler-0 and *p35S::GVG-6XUAS::LFY* transgenic plants in the absence of stimulation, in the presence of DMSO (mock), or 24 hours after the addition of dexamethasone (DEX) (n= 5 for each genotype and condition, $p = 0.0079$ Wilcoxon test). Data in A and B are expressed as the average and standard error.

(**C**) Expression of auxin biosynthetic genes *YUC1* and *YUC4* in plants of the indicated genotypes.

(**D**) Expression of auxin biosynthetic genes *TAA1* and *TAR2* in plants of the indicated genotypes. Data in C and D are normalized to the expression of *ACTIN2* and shown as the average and standard error of three experiments with 15–20 dissected shoot apices in each experiment. *p=0.028 Wilcoxon test.

(**E**) The relative amount of LFY transcript in *p35S::GVG-6XUAS::LFY* shoot apices exposed to 20 μM DEX or DMSO (mock treatment, 0.05% v/v) for 4, 12, 24, or 48 hours.

(**F**)The expression of *YUC1* in *p35S::GVG-6XUAS::LFY* shoot apices exposed to 20 μM DEX or DMSO (mock treatment) for 4 or 12 hours.

(**G**) The expression of *YUC4* in *p35S::GVG-6XUAS::LFY* shoot apices exposed to 20 μM DEX or DMSO (mock treatment) for 4 or 12 hours. Data in D–G are normalized to *ACTIN2* expression and shown as the average and standard error of three experiments with 15–20 shoot apices in each experiment.

(**H**) Yeast one-hybrid analysis of the binding of LFY to the *YUC4* gene. Genomic regions are indicated relative to the A in the start codon ATG, which is set at +1. Data shown are average and standard error of three experiments.

(**I**) The abundance of the endogenous *LFY* transcript *p35S::GVG-6XUAS::LFY* in shoot apices exposed to 20 μM DEX or DMSO (mock treatment) for 4 or 12 hours. Data are normalized to *ACTIN2* expression and shown as the average and standard error of three experiments with 15–20 shoot apices in each experiment.

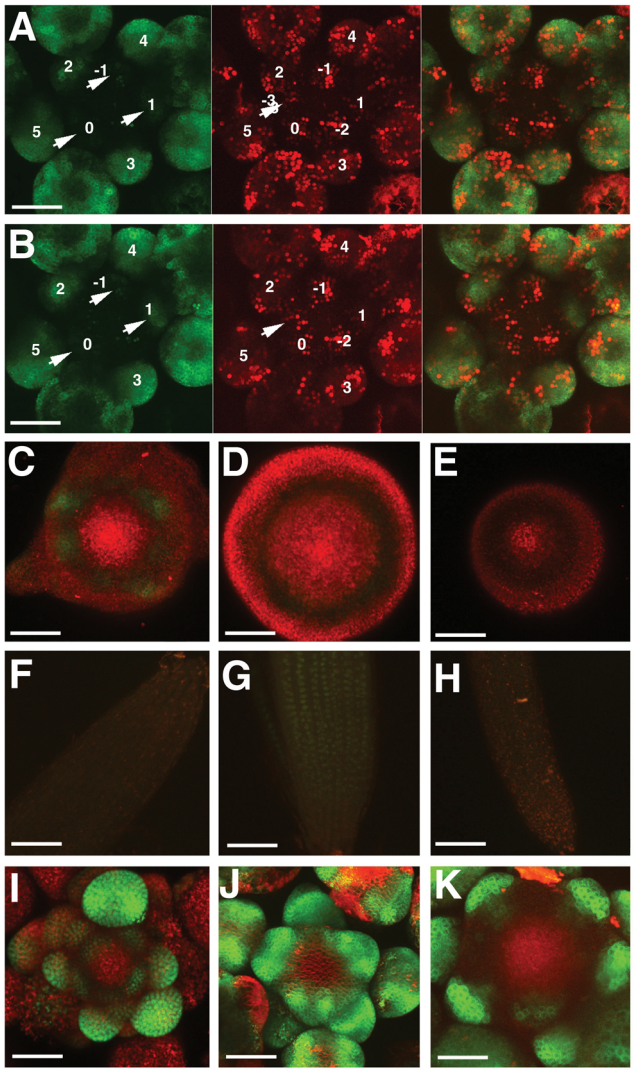

Fig. 3. Live imaging of a LFY reporter and a reporter of auxin signaling in developing floral buds. The LFY reporter is *pLFY::GFP-ER* (green) and the auxin signaling reporter is *pDR5rev::3XVenus-N7* (red)

(**A**) The LFY and DR5 reporters in Ler-0 SAM before DEX application (0 hours).

(**B**) The LFY and DR5 reporters in the same shoot apices imaged in A, but 6 hours later. The right panels in A and B are the overlay of the left and middle panels. Numbers in panels A and B indicate the sites of primordia with the larger numbers representing older primordia. Number 0 in the top panels indicates the sites of incipient primordia with the background intensity of LFY-GFP signal. Numbers are at the primordial regions unless with arrowheads in which cases the designated primordial sites are indicated with the arrowheads.

(**C**) The LFY and DR5 reporters in the *lfy-5 pid-8* double mutant plants.

(**D**) The LFY and DR5 reporters in *pin1-1* plants. The LFY reporter is barely detectable.

(**E**) The distribution of the LFY and DR5 reporters in *pid-4* plants which is a strong loss-of-function allele of PID. The LFY reporter is undetectable.

(**F**) The root of a plant with *pLFY::GFP-ER* under control buffer conditions. The LFY reporter is undetectable in the root epidermal and pith cells.

(**G**) The root of a plant with *pLFY::GFP-ER* plant after 24 hours growth on 10 μM NAA-supplemented media. LFY signal is detectable in the root epidermal and pith cells.
(**H**) The root of a plant with *pLFY::GFP-ER* plant pretreated with 10 μM cycloheximide and after 24 hours growth on 10 μM NAA. The LFY reporter is undetectable in the root epidermal and pith cells. In F–H, the LFY reporter is green; chlorophyll autofluorescence is red. Shown are the roots of 7-d old seedlings.
(**I**) The distribution of the LFY and DR5 reporters in Ler-0 SAMs. The LFY reporter is localized in floral primordia and developing floral buds.
(**J**) The distribution of the LFY and DR5 reporters in *lfy-5* SAMs.
(**K**) The distribution of the LFY and DR5 reporters in *pid-8* SAMs. Bars shown in all panels represent 50 μm.

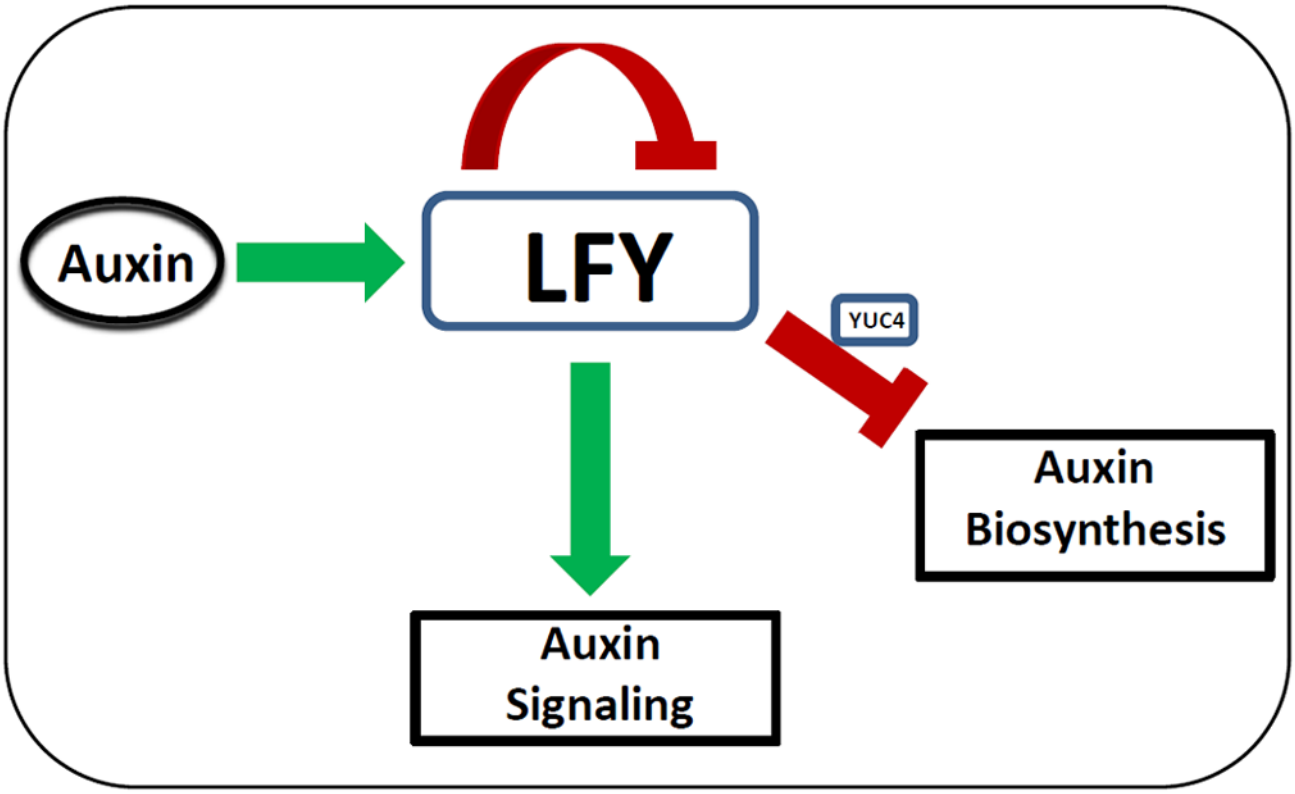

Fig. 4.

A model of LFY involvement in controlling auxin signaling in SAMs. Auxin promotes *LFY* expression, which stimulates auxin signaling, forming a positive feedback loop. However, LFY also inhibits its own expression and the expression of auxin biosynthesis genes (represented by *YUC4*) to provide negative input. Further work is needed to elucidate the components involved in other feedback regulation steps.